Recombinant kinesin motor domain binds to β-tubulin and decorates microtubules with a B surface lattice

(ATPase/chemical crosslinking/electron microscopy/flagella/optical diffraction)

YOUNG-HWA SONG AND ECKHARD MANDELKOW*

Max Planck Unit for Structural Molecular Biology, c/o Deutsches Elektronen Synchrotron, Notkestrasse 85, D-2000 Hamburg 52, Germany

ABSTRACT We have expressed the recombinant squid kinesin head domain in *Escherichia coli* and studied its interaction with microtubules. The head is active as a microtubule-stimulated ATPase and binds to microtubules, but it does not support microtubule gliding by itself. The head binds to both microtubules and depolymerized tubulin. In each case the zero-length crosslinker 1-ethyl-3-[3-(dimethylamino)propyl] carbodiimide induces a bond specifically to β- but not α-tubulin. The head decorates brain microtubules with an 8-nm axial spacing. Thus the stoichiometry is one kinesin head per tubulin dimer. The lattice is that of flagellar B-tubules, implying that reassembled microtubules are not symmetric. Moreover, the A- and B-tubules of intact flagellar outer doublets are both decorated with a B lattice. This suggests that the B lattice is a general property of microtubules.

Kinesin is the motor protein responsible for forward axonal transport (1, 2). It is a tetramer of two heavy and two light chains (3). The heavy chain consists of an N-terminal motor domain (the head) responsible for microtubule binding and ATP hydrolysis, a central stalk domain, and a C-terminal tail that is probably involved in light-chain and vesicle attachment (4, 5). These studies and several others (for recent reviews, see refs. 6–8) have defined some of the basic parameters of the motile machinery and opened the way to ask the following more-detailed questions. Does kinesin bind only to microtubules, or will it also interact with tubulin and other tubulin polymers? Since the building block of a microtubule is the α–β heterodimer, will kinesin bind to only one subunit or to both? Finally, can microtubules be decorated in a regular fashion with kinesin? If this is the case, what can we learn about the structure of microtubules and kinesin? The latter point is of particular importance in the microtubule field since there has been an ongoing debate on the surface lattice of microtubules.

These questions are difficult to address with native kinesin tetramers because of their size, heterogeneity, low yield, and other technical problems. Some of the problems can be circumvented by using just the kinesin head domain, prepared either by proteolytic cleavage (9) or by bacterial expression (10, 11). We have now expressed the recombinant squid kinesin head domain in *Escherichia coli*, starting from the kinesin heavy-chain clone of Kosik *et al.* (12). The head domain is ≈10% smaller than either of the tubulin chains and, therefore, well-suited for probing the interaction between tubulin monomers, dimers, or microtubules. In this paper, we show that the protein binds to depolymerized tubulin and microtubules and that only microtubules activate the ATPase. In both cases, the interaction appears to be with β-tubulin, as judged by chemical crosslinking. Consistent with this, the kinesin head decorates microtubules or other

polymers with the periodicity of the dimers, not the monomers. The lattice of the decorated polymers is typical of the B lattice, which implies that microtubules contain structural discontinuities.

MATERIALS AND METHODS

Preparation of Tubulin and Microtubules. Tubulin was purified by phosphocellulose chromatography after a microtubule-associated protein-depleting step as described (13). Microtubules were polymerized from phosphocellulose-purified tubulin by incubation at 37°C for 10–20 min in 0.1 M Pipes, pH 6.9/1 mM MgCl₂/1 mM EGTA/1 mM dithiothreitol/1 mM GTP (reassembly buffer). C-tubules (sheets) were polymerized in the same buffer supplemented with 1 M glycerol. Stabilization of microtubules was done with 20 μM taxol. Flagellar outer doublet microtubules were prepared from sea urchin sperm as described by Bell *et al.* (14); this disintegrates the flagellum and removes most of the nontubulin components.

Cloning and Expression of Kinesin Head. The coding sequence for the 395 N-terminal residues of squid kinesin heavy chain (12) was cloned in a derivative of the expression vector pET-3a (15), modified by deleting the original *Eco*RI site and introducing a new *Eco*RI site directly upstream of the termination signal of the T7 polymerase and by mutagenizing the *Nde* I site to a *Nco* I site. K. Kosik (Harvard Medical School, Boston) kindly provided clone 17A in which the truncated squid kinesin heavy-chain gene was cloned in the *Eco*RI site of the pUC19 vector. The truncated kinesin heavy-chain coding sequence was isolated from clone 17A by digestion with *Nco* I and *Eco*RI and inserted into the modified pET-3a vector at the same sites. For expression of the motor domain only, we deleted the sequences from *Spe* I to *Bam*HI site and generated a stop codon using a nonamer oligonucleotide (CTAGTTGAG). Plasmids were transformed into *E. coli* HMS174(DE3). Cells were harvested after 2 h of induction with 0.1 mM isopropyl β-D-thiogalactoside and lysed with a French press. Affinity purification of the high-speed supernatant (100,000 × g) was done with taxol-stabilized porcine brain microtubules in the presence of 0.5 mM adenosine 5′-[β,γ-imido]triphosphate (p[NH]ppA) or 2 mM PPP_i (2, 16). After incubation (10 min at 25°C) and pelleting (20 min at 100,000 × g), the kinesin head was dissociated from the microtubules with 10 mM MgATP. Further purification was done by Mono Q chromatography (Pharmacia; gradient, 0.15–1.0 M KCl). One gram (wet weight) of *E. coli* cells yields ≈1 mg of pure kinesin head.

Chemical Crosslinking. Kinesin and tubulin were crosslinked in reassembly buffer with 2 mM 1-ethyl-3-[3-(dimethylamino)propyl]carbodiimide and 5 mM *N*-hydroxysuccinimide for 30 min at room temperature (for microtu-

---

Abbreviation: p[NH]ppA, adenosine 5′-[β,γ-imido]triphosphate.
*To whom reprint requests should be addressed.

bules) or for 2 h at 4°C (for unpolymerized tubulin). The reaction was quenched by SDS sample buffer (17).

ATPase Assay. The ATPase assay was done as described by Seals *et al.* (18). Briefly, to 200 μl of kinesin head solution (0.4 mg/ml in reassembly buffer, with 1 M glycerol added) we added 10 μl of taxol-stabilized microtubules assembled from phosphocellulose-purified tubulin (16 mg/ml) so that the kinesin head was equimolar to tubulin dimer. The control without microtubules was done by adding 10 μl of buffer. To start the reaction, we added 1–100 μM MgATP including [γ-^{32}P]ATP with a specific activity of 6×10^{10} cpm/mol. After quenching the reaction, the inorganic phosphate was separated as a phosphomolybdate complex by organic-phase extraction [toluene/isobutanol, 1:1 (vol/vol)] and measured by scintillation counting.

Miscellaneous. Kinesin-induced motility of microtubules was observed by differential interference contrast video microscopy (2, 19), using a Zeiss IM35 microscope, a Hamamatsu Newvicon camera (C2400-01), and a Leutron Vision BM901 image processor (for details, see ref. 20). For electron microscopy, the specimens were negatively stained with 2% (wt/vol) uranyl acetate on carbon-coated grids and examined on a Philips CM12 microscope. Optical diffraction was done on a diffractometer equipped with a HeNe laser and an $f = 100$-cm lens. SDS/PAGE was performed on 0.5-mm slab gels with a polyacrylamide gradient from 4 to 20%. Immunoblot analysis was done on poly(vinylidene difluoride) membranes (Immobilon, Millipore). The bound antibody was detected by a peroxidase-conjugated second antibody (anti-rabbit or anti-mouse IgG, Dakopatts, Glostrup, Denmark). The following antibodies were used: polyclonal peptide antibody anti-H against kinesin head (21) and monoclonal antibodies DM1B against β-tubulin and DM1A against α-tubulin, both from Amersham.

RESULTS

Functions of Recombinant Kinesin Head. Fig. 1 illustrates the expression of the 395-residue squid kinesin head in *E. coli*. About 80–90% of the protein remained insoluble in inclusion bodies. The functional state of the soluble kinesin
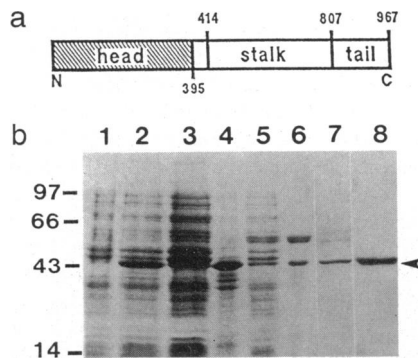

FIG. 1. (a) Diagram of 967-residue kinesin heavy chain (12) and its 395-residue head domain (hatched box). (b) Purification of the kinesin head domain (SDS/PAGE, 4–20% polyacrylamide gradient). Lanes: 1, total cell content after growing *E. coli* cells to an OD$_{600}$ value of 0.5 without induction; 2, total cell content 2 h after induction with 0.1 mM isopropyl β-D-thiogalactoside (note enhanced band at 43 kDa; arrowhead); 3 and 4, high-speed supernatant and pellet, respectively, of *E. coli* cells after French press lysis; 5 and 6, affinity purification of high-speed supernatant (see lane 3) with taxol-stabilized porcine brain microtubules; 7, dissociation of kinesin head by ATP. The pellet (lane 6) was resuspended in microtubule-stabilizing buffer including 10 mM MgATP and pelleted as before. Most of the kinesin remains in the supernatant. Lane 8 shows the purification of the supernatant (see lane 7) on a Mono Q column. Molecular mass markers are on the left in kDa.

was assessed by three criteria, the binding to microtubules, the ATPase activity, and the motility. The binding to microtubules is most pronounced in the presence of the ATP analog p[NH]ppA because this induces a "rigor-like" state (1, 2). The recombinant squid kinesin head exhibited the same behavior; this allowed its purification from the bacterial extracts (Fig. 1b) and provided the basis for the structural studies described below. The bound kinesin head could be released again by adding ATP.

The ATPase activity of purified kinesin head was very low, with a V_{max} value on the order of 10 sec^{-1}. However, it could be enhanced 10-fold or more by the addition of taxol-stabilized microtubules. This is comparable to intact kinesin (3, 16, 22). The K_m values are ≈5 μM in both cases (data not shown).

Whereas the ATPase and microtubule binding properties were as expected, the squid kinesin head did not cause microtubules to attach or to move on the glass surface (data not shown). This is similar to observations on bovine and *Drosophila* kinesin head (9, 10); it indicates that a motor domain needs part of the stalk for force transduction.

Crosslinking of Kinesin Head to β-Tubulin. Tubulin subunits consist of heterodimers of α- and β-tubulin so that one may ask whether kinesin binds to one subunit or both subunits. We approached this question by crosslinking with the zero-length crosslinker 1-ethyl-3-[3-(dimethylamino)propyl]carbodiimide and identifying the adducts with specific antibodies (Fig. 2). The results show that kinesin head is crosslinked to β-tubulin (Fig. 2b, lanes 1 and 3) but not to α-tubulin (Fig. 2c). The simplest interpretation is that kinesin binds to β-tubulin only; this would be consistent with the structural results presented below. It is also possible that the kinesin head binds to the interface between α- and β-tubulin and that a crosslink is formed only with β-tubulin. However, we can rule out the possibility that α- and β-tubulin both bind
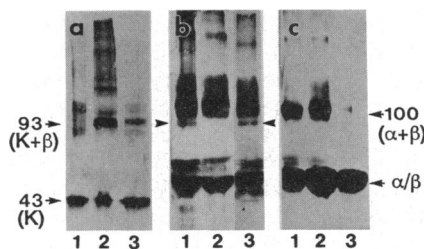
FIG. 2. Crosslinking of kinesin head to β-tubulin by 1-ethyl-3-[3-(dimethylamino)propyl]carbodiimide shown on immunoblots. The following antibodies were used. (a) Anti-H against kinesin head (21). (b) DM1B against β-tubulin. (c) DM1A against α-tubulin. (a) Lanes: 1, crosslinking of kinesin head alone (0.5 mg/ml); 2, kinesin head (0.5 mg/ml)/microtubules (made from phosphocellulose-purified tubulin at 2.5 mg/ml and stabilized with 20 μM taxol)/0.5 mM p[NH]ppA; 3, kinesin head (0.5 mg/ml)/phosphocellulose-purified tubulin (2.5 mg/ml)/0.5 mM p[NH]ppA. (b and c) Lanes: 1, crosslinking of kinesin head and taxol-stabilized microtubules; 2, taxol-stabilized microtubules (control without kinesin head); 3, kinesin head/phosphocellulose-purified tubulin. (a) Kinesin itself is only poorly crosslinked. Lane 1 shows kinesin monomer (K) at 43 kDa and dimer at ≈80 kDa. Lane 2 shows kinesin head monomer (43 kDa) and a strong band at 93 kDa. This band is the kinesin head–β-tubulin complex (K+β; see also b). The high molecular weight bands are presumably the higher-order complexes of kinesin head and β-tubulin. (b) Blot with anti-β-tubulin, showing the presence of β-tubulin in the 93-kDa adduct (arrowheads) and in the crosslinked tubulin dimer at ≈100 kDa. The bands >100 kDa could be either crosslinked homo- or heterodimers of α- and β-tubulin (23) or higher-order complexes of kinesin head and β-tubulin. (c) Blot with anti-α-tubulin, showing that α-tubulin is absent from the 93-kDa adduct. These data show that the kinesin head binds to microtubules (a, lane 2; b and c, lanes 1) and to unpolymerized tubulin (a and b, lanes 3) and is specifically crosslinked to β-tubulin.

Biochemistry: Song and Mandelkow

Proc. Natl. Acad. Sci. USA 90 (1993) 1673
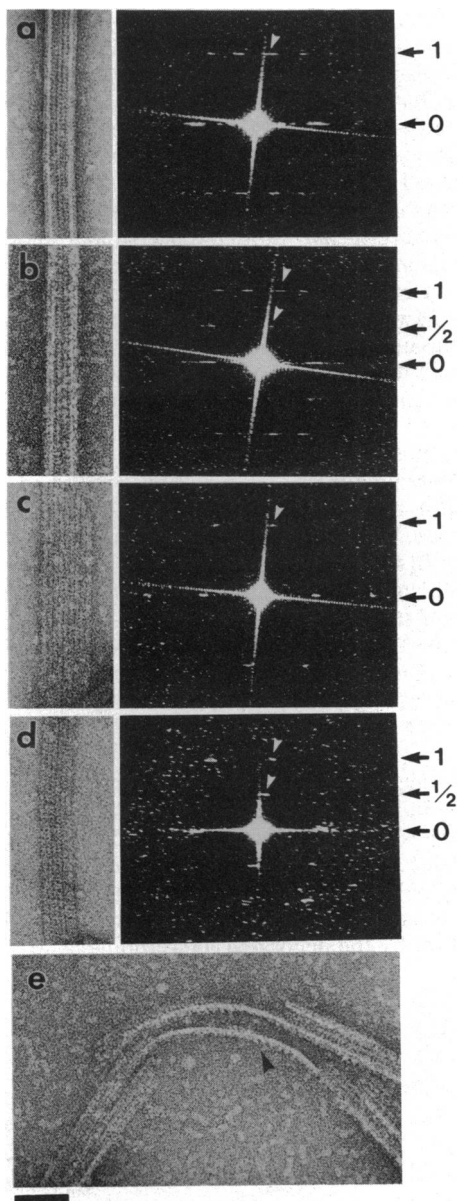
FIG. 3. Electron micrographs (*Left*) and diffraction patterns (*Right*) of microtubules and sheets decorated with kinesin head. Numbers on the right are layer-line indices, based on the tubulin monomer repeat of 4 nm (line 1, 4-nm layer line; line ½, 8-nm layer line). The bright cross is the diffraction from the mask and of no importance here. (*a*) Microtubule without kinesin head decoration (control), showing the typical longitudinal protofilaments. The diffraction pattern shows a clear layer line corresponding to the 4-nm axial repeat of tubulin monomers. The inner pair of reflections (symmetric about the meridian) represent the J_3 Bessel terms arising from the front and back of the microtubule; the outer pair is from the J_{10} term (for details see ref. 24). There is no 8-mm layer line because the contrast between α- and β-tubulin is too weak. (*b*) Decorated microtubule. Note the oblique cross-striations spaced 8 nm axially and inclined ≈10° to the horizontal. The optical diffraction pattern contains an 8-nm layer line. The spot indicated by an arrowhead is halfway between the origin and the J_3 spot on the 4-nm layer line (arrowhead), indicating a B lattice. The layer line is one-sided due to uneven staining. In contrast, there is no reflection halfway toward the J_{10} spot, which would be expected from the A lattice. (*c*) Sheet (single-layered microtubule wall) without decoration showing protofilaments (*Left*) and a 4-nm layer line. In this case the layer line is asymmetric because the microtubule wall is seen in only one orientation (for details, see ref. 25). (*d*) Decorated sheet showing oblique cross-striations at 8-nm spacing. The corresponding diffraction spot is halfway toward the J_3 spot, indicating the B lattice (see arrow-

kinesin heads simultaneously since this would not be compatible with the surface lattice (see below).

Another question is whether kinesin binding depends on the assembly state of tubulin. It is known that the activation of the kinesin ATPase requires assembled microtubules (16). This could mean either that the activation is due to several tubulin subunits acting in concert or that a certain conformation of the assembled state is required. When we probed kinesin binding in the presence of p[NH]ppA, we found that the head was crosslinked both to microtubules and to depolymerized tubulin (and in both cases to β-tubulin; Fig. 2 *a*, lanes 2 and 3, and *b*, lanes 1 and 3). This suggests that the kinesin head can associate with a single tubulin dimer and that binding and activation of ATPase are two separate aspects of the kinesin–tubulin interaction.

Decoration of the Microtubule Lattice by Kinesin Head. Next we asked how the kinesin head binds to the microtubule lattice. Fig. 3 shows that this takes place in a periodic fashion. Tubulin dimers have an 8-nm repeat along protofilaments, but the predominant contrast comes from the monomers and gives rise to a 4-nm layer line (labeled line 1 in Fig. 3). The 8-nm periodicity is strongly enhanced by the bound kinesin head (compare Fig. 3 *a* and *b*). In the image the decoration can be seen as cross-striations inclined ≈10° to the horizontal (Fig. 3*b Left*). In the optical diffraction pattern, this gives rise to an 8-nm layer line that is normally absent due to the low contrast between α- and β-tubulin (labeled line ½ in Fig. 3). This shows that each tubulin dimer binds only one kinesin head, not two. This means that the kinesin decoration can be used to identify the lattice of tubulin dimers in microtubules.

One of the most intriguing results is the position of the reflections on the 8-nm layer line. There is a near-meridional spot midway between the origin and the J_3 reflection on the 4-nm layer line (Fig. 3*b*, arrowheads). This is typical of the B-lattice reported for flagellar outer doublets [for details on the analysis, see Amos and Klug (24)]. It means that the tubulin dimers are aligned along the shallow 3-start helix (see Fig. 5 *b* and *c*). The analysis can be simplified if one uses tubulin sheets—i.e., incomplete microtubule walls flattened on the grid (Fig. 3 *c* and *d*). In this case, one observes the microtubule wall in only one orientation, rather than the superposition of front and back. Again the kinesin head decoration was at ≈10° inclination and had an 8-nm axial repeat, with a corresponding 8-nm layer line in the diffraction pattern, confirming the B-lattice (Fig. 3*d*, arrowheads). Fig. 3*e* shows microtubule walls in projection and illustrates that the kinesin head particles are indeed attached to the outside and project ≈5 nm from the surface.

The distinction of A and B lattices was originally derived from images of A- and B-tubules of flagellar outer doublets that still contained nontubulin components, noticeable by the low-angle layer lines (24). We therefore wanted to check whether flagellar doublets largely freed of nontubulin components could be decorated by kinesin head. This is indeed the case (Fig. 4 *Left*). Diffraction patterns taken from the individual microtubules showed 8-nm layer lines with the reflections compatible with the B-lattice but not the A-lattice (Fig. 4 *Middle* and *Right*). This means that the A- and B-tubules have the B surface lattice and suggests that the A lattice described by Amos and Klug (24) may have been mimicked by nontubulin components [as suggested by Linck and Langevin (27)].

heads), but there is no spot halfway toward the J_{10} spot. (*e*) Decorated microtubule opening up and folding over on the grid. Kinesin head molecules are contrasted in projection on the outside surface. The axial spacing between the heads is ≈8 nm, and they project ≈5 nm from the surface. (Bar = 50 nm.)
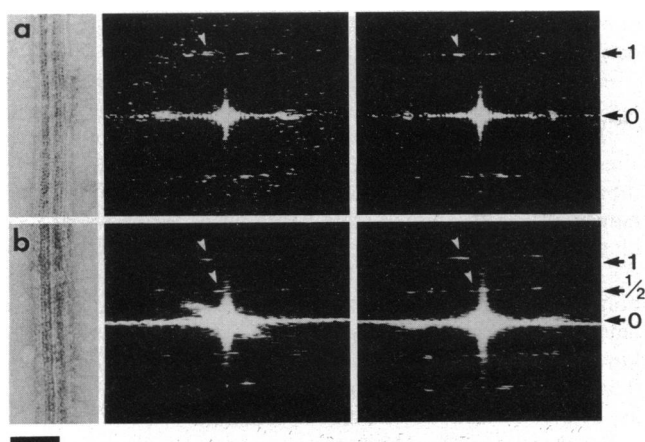
FIG. 4. Flagellar outer doublets (*Left*) and diffraction patterns of the individual tubules (*Middle* and *Right*). (*a*) Control without decoration. (*b*) Decorated with kinesin head. Because the nontubulin components were removed, the low-angle layer lines typical of intact flagellar microtubules have disappeared (for comparison, see refs. 24 and 26). Only the decorated microtubules show an 8-nm layer line (at the bottom), with reflections in positions corresponding to the B lattice (arrowheads).

DISCUSSION

In this study we used the bacterially expressed squid kinesin head to address several questions on the interaction of microtubules, tubulin, and kinesin. The head domain behaves as expected in that it binds to microtubules in the presence of p[NH]ppA, it has a microtubule-activated ATPase, and it can be released from microtubules by ATP. Other preparations of kinesin head have been reported in the literature. For example, Kuznetsov *et al.* (9) used proteolytically cleaved head domains from bovine brain and found $V_{max} \approx$ 60–90 sec^{-1} and $K_m \approx$ 75–100 μM. Gilbert and Johnson (11) reported on a recombinant kinesin head from *Drosophila* with $V_{max} =$ 5.7 sec^{-1} and $K_m =$ 3 μM, and Harrison *et al.* (28) showed that this protein also bound to microtubules in an ATP-reversible manner. Considering the differences in species, protein size, or possible effects of posttranslational modifications, these observations are in good agreement with ours. A special point is that our kinesin head will not support microtubule gliding, similar to the results of Kuznetsov *et al.* (9). Yang *et al.* (10) have explained this by noting that the motility requires a piece of the kinesin stalk or equivalent protein to transduce the force produced by the head.

One open question was whether kinesin binds to one or both tubulin monomers and whether the binding depends on the assembly state. The answer is that one tubulin dimer binds one kinesin head. The crosslinking results show that the target for binding is probably β-tubulin, although we cannot strictly exclude the possibility that kinesin binds to the interface between α- and β-tubulin and that the crosslink happens to stabilize only the bond to β-tubulin. This leads to some interesting conclusions. Kirchner and Mandelkow (23) have shown that the intradimer bond of tubulin is formed by the C-terminal domain of β-tubulin and the N-terminal domain of α-tubulin. It seems also clear that motor proteins such as kinesin or dynein interact with the C-terminal domain of tubulin (29–31). Thus, if the kinesin head interacts with β-tubulin, then it would be near the N-terminal domain of α-tubulin—i.e., around the internal region of the dimer that is presumably not affected by assembly. Consistent with this, we find that the binding to β-tubulin occurs in the assembled and disassembled state.

There is currently a debate regarding the details of the binding site of microtubule-associated proteins and motors.

Paschal *et al.* (29) have placed the interaction site with dynein very near the C terminus; Rodionov *et al.* (30) and Goldsmith *et al.* (31) place it further inward, in the vicinity of residues 420–430. Our present data do not speak to these results directly, but it is worth noting that the β-tubulin peptide containing residues β400–436 inhibits both dynein-based and kinesin-based motility (31). Goldsmith *et al.* (31) subdivide the C-terminal domain into three regions, region I (residues 400–412) where α- and β-tubulin are similar and both conserved, region II (residues 412–426) where they are distinct yet still conserved within their class, and region III (beyond residue 426) where both are very heterogeneous. Because of this they argue that the binding of motors—which should be a conserved feature—should be in regions I or II. Our data would be consistent with kinesin binding to region II of β-tubulin.

Perhaps the most puzzling feature of microtubules is the lattice of tubulin dimers. This can now be studied in a direct way because the bound kinesin enhances the contrast of the dimer lattice. Two models have been proposed for microtubules (24): In the B lattice the dimers are in register along the 3-start helix (as in Fig. 5 *b* and *c*) and in the A lattice they are roughly half-staggered (Fig. 5*a*). These lattices were thought to occur in flagellar B- and A-tubules, respectively. An important point is that only the A lattice generates a symmetric microtubule of 13 protofilaments. It was therefore assumed that cytoplasmic microtubules should have the A lattice.

Direct evidence for this was very difficult to obtain because α- and β-tubulin are hard to distinguish by diffraction methods. There were, however, several indications that brain microtubules had a B lattice. They were obtained by x-ray scattering (33) or by electron microscopy and image reconstruction of microtubules or polymorphic forms (34–36). We now confirm by the decorated microtubules and sheets that
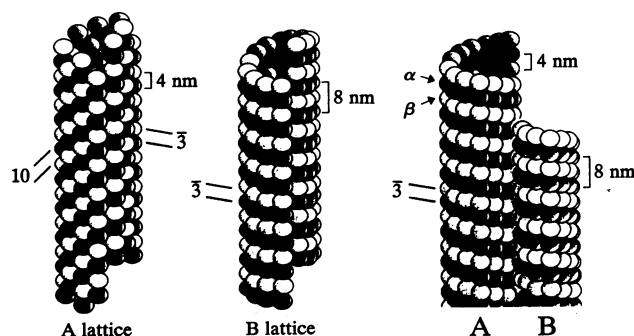

FIG. 5. Models of singlet and doublet microtubules with different surface lattices of tubulin dimers (following ref. 24). In each microtubule, α-tubulin is shaded darkly and β-tubulin is shaded more lightly. (*a*) Single microtubule with A lattice. The dimers in adjacent protofilaments are staggered by 3.1 nm, generating a checkered appearance. This lattice is not compatible with the data on kinesin decoration. (*b*) Single microtubule with B lattice where adjacent dimers are staggered by only 0.9 nm, giving a more banded appearance. The bands slope gently up and to the left, following a 3-start helix (as indicated). Thus the lattice lines with 4-nm and 8-nm spacing point in the same direction. This feature generates the near-meridional reflection on the 8-nm layer line in Fig. 3 *b* and *d*. Note, however, that in this lattice the helical lines must be interrupted by a discontinuity where dark subunits switch to light ones shown in front. The B lattice is the only one we have observed experimentally. (*c*) Flagellar outer doublet microtubule. The two tubules are distinguished by different shading, but both the A- and B-tubule have a B lattice. The direction of the 3-start helix is shown on left (note that both the monomers and the dimers are aligned along the same direction). The discontinuity is hidden behind the right edge of the A-tubule. Note that in each case the microtubules terminate with α-subunits at one end and β-subunits at the other.

Biochemistry: Song and Mandelkow

Proc. Natl. Acad. Sci. USA 90 (1993) 1675

brain microtubules have a B lattice (Fig. 3). This implies that microtubules cannot be helically symmetric, they must have a seam (facing the observer in Fig. 5*b*) or some other discontinuity (32).

One could argue that the microtubules shown in Fig. 3 had been disassembled and reassembled and that this could have altered the lattice artificially. We therefore turned to flagellar doublet microtubules that were prepared without disassembly. The 8-nm reflections are less pronounced because of close juxtaposition of the two microtubules, but they are consistent only with the B lattice and not with the A lattice. This is true for both microtubules; in other words, both the A- and the B-microtubules of flagellar outer doublets have the B lattice.

The question arises whether the A lattice exists at all. Although it is difficult to generalize, this seems unlikely. We think it is more probable to assume that all microtubules have the same surface lattice, the B lattice. In the original Amos and Klug study (24), reflections pointing to the A lattice could have arisen from microtubule-associated proteins. This would be consistent with the Linck and Langevin (27) study on purified flagellar microtubules. A model of a flagellar doublet is presented in Fig. 5*c*. The main feature is that the tubulin dimers are aligned along the 3-start helices in both tubules. The structure implies that both microtubules are discontinuous. For the B-tubule this is not a problem since it is incomplete anyway. For the A-tubule the location of the discontinuity is unknown and hidden in the diagram. Similarly, the stagger between the two microtubules is unknown and chosen arbitrarily.

The model could be a starting point for a refined investigation of the structure of flagellar tubules and their interactions with motor proteins. For example, Gelles *et al.* (37) observed 4-nm steps in the movement of kinesin-coated beads along microtubules, and Kamimura and Kamiya (38) showed that dynein-induced flagellar motion has step sizes reflecting both the monomer and dimer spacings (i.e., 4-nm and 8-nm components). Both examples suggest that tubulin monomers are somehow important in motility. One could hypothesize that kinesin can touch down transiently on either tubulin isotype during ATP-driven motion, even though it prefers β-tubulin in the rigor state (with p[NH]ppA). Alternatively, the two heads of native kinesin might work differently than just one. Finally, Kamimura and Mandelkow (39) noted that the speed of kinesin-coated beads did not change when they passed from a flagellar outer doublet to a singlet microtubule extending from the A-tubule. At the time the result was thought to mean that kinesin did not sense the difference between surface lattices. The present results make the interpretation even simpler since the dimer lattices are the same for A- and B-tubules.

1. Brady, S. T. (1985) *Nature (London)* **317**, 73–75.
2. Vale, R. D., Reese, T. S. & Sheetz, M. P. (1985) *Cell* **42**, 39–50.
3. Bloom, G., Wagner, M., Pfister, K. & Brady, S. (1988) *Biochemistry* **27**, 3409–3416.
4. Scholey, J., Heuser, J., Yang, J. & Goldstein, L. (1989) *Nature (London)* **338**, 355–357.
5. Yang, J., Laymon, R. & Goldstein, L. (1989) *Cell* **56**, 879–889.
6. Vallee, R. & Shpetner, H. (1990) *Annu. Rev. Biochem.* **59**, 909–932.
7. Goldstein, L. S. B. (1991) *Trends Cell Biol.* **1**, 93–98.
8. Bloom, G. S. (1992) *Curr. Opin. Cell Biol.* **4**, 66–73.
9. Kuznetsov, S., Vaisberg, Y., Rothwell, S., Murphy, D. & Gelfand, V. I. (1989) *J. Biol. Chem.* **264**, 589–595.
10. Yang, J. T., Saxton, W., Stewart, R., Raff, E. & Goldstein, L. (1990) *Science* **249**, 42–47.
11. Gilbert, S. P. & Johnson, K. A. (1991) *J. Cell Biol.* **115**, 388a (abstr.).
12. Kosik, K., Orecchio, L., Schnapp, B., Inouye, H. & Neve, R. (1990) *J. Biol. Chem.* **265**, 3278–3283.
13. Mandelkow, E.-M., Herrmann, M. & Rühl, U. (1985) *J. Mol. Biol.* **185**, 311–327.
14. Bell, C., Fraser, C., Sale, W., Tang, W.-J. & Gibbons, I. R. (1982) *Methods Cell Biol.* **24**, 373–397.
15. Studier, W. F., Rosenberg, A. H., Dunn, J. J. & Dubendorff, J. W. (1990) *Methods Enzymol.* **185**, 60–89.
16. Kuznetsov, S. & Gelfand, V. (1986) *Proc. Natl. Acad. Sci. USA* **83**, 8530–8534.
17. Staros, J., Wright, R. & Swingle, D. (1986) *Anal. Biochem.* **156**, 220–222.
18. Seals, J. R., McDonald, J. M., Bruns, D. & Jarett, L. (1978) *Anal. Biochem.* **90**, 785–795.
19. Allen, R., Weiss, D., Hayden, J., Brown, D., Fujiwake, H. & Simpson, M. (1985) *J. Cell Biol.* **100**, 1736–1752.
20. Von Massow, A., Mandelkow, E.-M. & Mandelkow, E. (1989) *Cell Motil. Cytoskel.* **14**, 562–571.
21. Sawin, K. E., Mitchison, T. J. & Wordeman, L. G. (1992) *J. Cell Sci.* **101**, 303–313.
22. Hackney, D. (1988) *Proc. Natl. Acad. Sci. USA* **85**, 6314–6318.
23. Kirchner, K. & Mandelkow, E. (1985) *EMBO J.* **4**, 2397–2402.
24. Amos, L. A. & Klug, A. (1974) *J. Cell Sci.* **14**, 523–549.
25. Erickson, H. P. (1974) *J. Cell Biol.* **60**, 153–167.
26. Murray, J. M. (1991) *Int. Rev. Cytol.* **125**, 47–93.
27. Linck, R. W. & Langevin, G. L. (1981) *J. Cell Biol.* **89**, 323–337.
28. Harrison, B. C., Marchese-Ragona, S. & Johnson, K. A. (1991) *J. Cell Biol.* **115**, S45 (abstr.).
29. Paschal, B., Obar, R. & Vallee, R. (1989) *Nature (London)* **342**, 569–572.
30. Rodionov, V., Gyoeva, F., Kashina, A., Kuznetsov, S. & Gelfand, V. (1990) *J. Biol. Chem.* **265**, 5702–5707.
31. Goldsmith, M., Connolly, J., Kumar, N., Wu, J., Yarbrough, L. & Vanderkooy, D. (1991) *Cell Motil. Cytoskel.* **20**, 249–262.
32. Mandelkow, E.-M., Schultheiss, R., Rapp, R., Müller, M. & Mandelkow, E. (1986) *J. Cell Biol.* **102**, 1067–1073.
33. Mandelkow, E., Thomas, J. & Cohen, C. (1977) *Proc. Natl. Acad. Sci. USA* **74**, 3370–3374.
34. Mandelkow, E. M., Mandelkow, E., Unwin, P. N. T. & Cohen, C. (1977) *Nature (London)* **265**, 655–657.
35. Crepeau, R. H., McEwen, B. & Edelstein, S. J. (1978) *Proc. Natl. Acad. Sci. USA* **75**, 5006–5010.
36. McEwen, B. & Edelstein, S. (1980) *J. Mol. Biol.* **139**, 123–145.
37. Gelles, J., Schnapp, B. & Sheetz, M. (1988) *Nature (London)* **331**, 450–453.
38. Kamimura, S. & Kamiya, R. (1992) *J. Cell Biol.* **116**, 1443–1454.
39. Kamimura, S. & Mandelkow, E. (1992) *J. Cell Biol.* **118**, 865–875.